

Detection of the ISW effect and corresponding dark energy constraints

J. D. McEwen¹, P. Vielva^{2,3}, M. P. Hobson¹,
E. Martínez-González², A. N. Lasenby¹, J. Delabrouille³

¹Astrophysics Group
University of Cambridge

²Instituto de Física de Cantabria
Universidad de Cantabria

³Laboratoire APC
Collège de France

15 November 2005

Outline

- 1 Integrated Sachs-Wolfe (ISW) effect
 - Physical origin
 - Detecting the effect
- 2 The continuous spherical wavelet transform (CSWT)
 - Dilations and mother wavelets on the sphere
 - Transform
- 3 Cross-correlation in wavelet space
 - Wavelet covariance estimator
 - Comparison of wavelets
- 4 Analysis procedure
- 5 Results
 - Detections
 - Dark energy constraints
- 6 Summary

Outline

- 1 Integrated Sachs-Wolfe (ISW) effect
 - Physical origin
 - Detecting the effect
- 2 The continuous spherical wavelet transform (CSWT)
 - Dilations and mother wavelets on the sphere
 - Transform
- 3 Cross-correlation in wavelet space
 - Wavelet covariance estimator
 - Comparison of wavelets
- 4 Analysis procedure
- 5 Results
 - Detections
 - Dark energy constraints
- 6 Summary

ISW effect

Physical origin

- Photons blue (red) shifted when fall into (out of) potential wells
- Evolution of potential during photon propagation
→ net change in photon energy
- Large scale phenomenon
(cosmic variance limited → require full-sky maps)
- Only present in non-flat universes or flat universes with dark energy

Temperature perturbation

$$\frac{\delta T}{T} = 2 \int \frac{\dot{\Phi}}{c^2} \frac{d\ell}{c}$$

where $d\ell$ is the element of proper distance. In Einstein de-Sitter universe (no Λ), $\Phi_k \sim \delta_k/a$ and linear growth law for $\Omega = 1$ is $\delta_k \sim a$. Thus $\dot{\Phi} \neq 0$ only when Ω diverges significantly from unity.

ISW effect

Physical origin

- Photons blue (red) shifted when fall into (out of) potential wells
- Evolution of potential during photon propagation
→ net change in photon energy
- Large scale phenomenon
(cosmic variance limited → require full-sky maps)
- Only present in non-flat universes or flat universes with dark energy

Temperature perturbation

$$\frac{\delta T}{T} = 2 \int \frac{\dot{\Phi}}{c^2} \frac{d\ell}{c}$$

where $d\ell$ is the element of proper distance. In Einstein de-Sitter universe (no Λ), $\Phi_k \sim \delta_k/a$ and linear growth law for $\Omega = 1$ is $\delta_k \sim a$. Thus $\dot{\Phi} \neq 0$ only when Ω diverges significantly from unity.

ISW effect

Physical origin

- Photons blue (red) shifted when fall into (out of) potential wells
- Evolution of potential during photon propagation
→ net change in photon energy
- Large scale phenomenon
(cosmic variance limited → require full-sky maps)
- Only present in non-flat universes or flat universes with dark energy

Temperature perturbation

$$\frac{\delta T}{T} = 2 \int \frac{\dot{\Phi}}{c^2} \frac{d\ell}{c}$$

where $d\ell$ is the element of proper distance. In Einstein de-Sitter universe (no Λ), $\Phi_k \sim \delta_k/a$ and linear growth law for $\Omega = 1$ is $\delta_k \sim a$. Thus $\dot{\Phi} \neq 0$ only when Ω diverges significantly from unity.

ISW effect

Physical origin

- Photons blue (red) shifted when fall into (out of) potential wells
- Evolution of potential during photon propagation
→ net change in photon energy
- Large scale phenomenon
(cosmic variance limited → require full-sky maps)
- Only present in non-flat universes or flat universes with dark energy

Temperature perturbation

$$\frac{\delta T}{T} = 2 \int \frac{\dot{\Phi}}{c^2} \frac{d\ell}{c}$$

where $d\ell$ is the element of proper distance. In Einstein de-Sitter universe (no Λ), $\Phi_k \sim \delta_k/a$ and linear growth law for $\Omega = 1$ is $\delta_k \sim a$. Thus $\dot{\Phi} \neq 0$ only when Ω diverges significantly from unity.

Detecting the ISW effect

Cross-correlating the CMB with LSS

- Cannot directly separate the ISW signal from CMB anisotropies
- Detected by cross-correlating CMB anisotropies with tracers of large scale structure
(first proposed by Crittenden & Turok 1996)
- Detections used to place constraints on dark energy
- Previous works
 - Real space angular correlation function
(e.g. Boughn & Crittenden 2002)
 - Harmonic space cross-angular power spectrum
(e.g. Afshordi et al. 2004)
 - Wavelet space covariance (Vielva et al. 2005)
- We extend spherical wavelet approach to directional wavelets (no reason to expect azimuthally symmetric structures)

Detecting the ISW effect

Cross-correlating the CMB with LSS

- Cannot directly separate the ISW signal from CMB anisotropies
- Detected by cross-correlating CMB anisotropies with tracers of large scale structure
(first proposed by Crittenden & Turok 1996)
- Detections used to place constraints on dark energy
- Previous works
 - Real space angular correlation function
(e.g. Boughn & Crittenden 2002)
 - Harmonic space cross-angular power spectrum
(e.g. Afshordi et al. 2004)
 - Wavelet space covariance (Vielva et al. 2005)
- We extend spherical wavelet approach to directional wavelets (no reason to expect azimuthally symmetric structures)

Detecting the ISW effect

Cross-correlating the CMB with LSS

- Cannot directly separate the ISW signal from CMB anisotropies
- Detected by cross-correlating CMB anisotropies with tracers of large scale structure
(first proposed by Crittenden & Turok 1996)
- Detections used to place constraints on dark energy
- Previous works
 - Real space angular correlation function
(e.g. Boughn & Crittenden 2002)
 - Harmonic space cross-angular power spectrum
(e.g. Afshordi et al. 2004)
 - Wavelet space covariance (Vielva et al. 2005)
- We extend spherical wavelet approach to directional wavelets (no reason to expect azimuthally symmetric structures)

Detecting the ISW effect

Cross-correlating the CMB with LSS

- Cannot directly separate the ISW signal from CMB anisotropies
- Detected by cross-correlating CMB anisotropies with tracers of large scale structure
(first proposed by Crittenden & Turok 1996)
- Detections used to place constraints on dark energy
- Previous works
 - Real space angular correlation function
(e.g. Boughn & Crittenden 2002)
 - Harmonic space cross-angular power spectrum
(e.g. Afshordi et al. 2004)
 - Wavelet space covariance (Vielva et al. 2005)
- We extend spherical wavelet approach to directional wavelets (no reason to expect azimuthally symmetric structures)

Detecting the ISW effect

Cross-correlating the CMB with LSS

- Cannot directly separate the ISW signal from CMB anisotropies
- Detected by cross-correlating CMB anisotropies with tracers of large scale structure
(first proposed by Crittenden & Turok 1996)
- Detections used to place constraints on dark energy
- Previous works
 - Real space angular correlation function
(e.g. Boughn & Crittenden 2002)
 - Harmonic space cross-angular power spectrum
(e.g. Afshordi et al. 2004)
 - Wavelet space covariance (Vielva et al. 2005)
- We extend spherical wavelet approach to directional wavelets (no reason to expect azimuthally symmetric structures)

Outline

- 1 Integrated Sachs-Wolfe (ISW) effect
 - Physical origin
 - Detecting the effect
- 2 **The continuous spherical wavelet transform (CSWT)**
 - Dilations and mother wavelets on the sphere
 - Transform
- 3 Cross-correlation in wavelet space
 - Wavelet covariance estimator
 - Comparison of wavelets
- 4 Analysis procedure
- 5 Results
 - Detections
 - Dark energy constraints
- 6 Summary

Spherical wavelet transform

Anisotropic dilation on the sphere

- Spherical wavelet transform (Antoine and Vandergheynst 1998; Wiaux et al. 2005)
- Stereographic projection Π
- Anisotropic dilation on the sphere

$$\mathcal{D}(a, b) = \Pi^{-1} d(a, b) \Pi$$

$$[\mathcal{D}(a, b)s](\omega) = [\lambda(a, b, \theta, \phi)]^{1/2} s(\omega_{1/a, 1/b})$$

where

$$\omega_{a,b} = (\theta_{a,b}, \phi_{a,b}),$$

$$\tan(\theta_{a,b}/2) = \tan(\theta/2) \sqrt{a^2 \cos^2 \phi + b^2 \sin^2 \phi}$$

$$\tan(\phi_{a,b}) = \frac{b}{a} \tan(\phi)$$

Spherical wavelet transform

Anisotropic dilation on the sphere

- Spherical wavelet transform (Antoine and Vandergheynst 1998; Wiaux et al. 2005)
- Stereographic projection Π
- Anisotropic dilation on the sphere

$$\mathcal{D}(a, b) = \Pi^{-1} d(a, b) \Pi$$

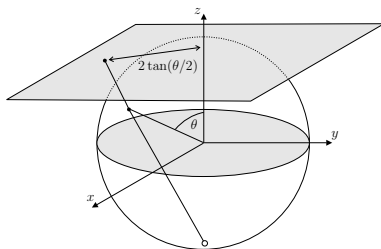
$$[\mathcal{D}(a, b)s](\omega) = [\lambda(a, b, \theta, \phi)]^{1/2} s(\omega_{1/a, 1/b})$$

where

$$\omega_{a,b} = (\theta_{a,b}, \phi_{a,b}),$$

$$\tan(\theta_{a,b}/2) = \tan(\theta/2) \sqrt{a^2 \cos^2 \phi + b^2 \sin^2 \phi}$$

$$\tan(\phi_{a,b}) = \frac{b}{a} \tan(\phi)$$



Spherical wavelet transform

Anisotropic dilation on the sphere

- Spherical wavelet transform (Antoine and Vandergheynst 1998; Wiaux et al. 2005)
- Stereographic projection Π
- Anisotropic dilation on the sphere

$$\mathcal{D}(a, b) = \Pi^{-1} d(a, b) \Pi$$

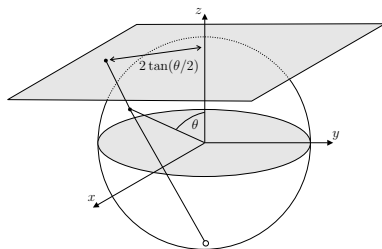
$$[\mathcal{D}(a, b)s](\omega) = [\lambda(a, b, \theta, \phi)]^{1/2} s(\omega_{1/a, 1/b})$$

where

$$\omega_{a,b} = (\theta_{a,b}, \phi_{a,b}),$$

$$\tan(\theta_{a,b}/2) = \tan(\theta/2) \sqrt{a^2 \cos^2 \phi + b^2 \sin^2 \phi}$$

$$\tan(\phi_{a,b}) = \frac{b}{a} \tan(\phi)$$



Spherical wavelet transform

Mother wavelets on the sphere

- Stereographic projection of admissible Euclidean mother wavelets

$$\psi(\omega) = [\Pi^{-1}\psi_{\mathbb{R}^2}](\omega)$$

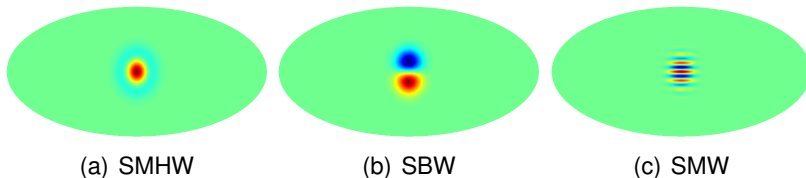


Figure: Spherical wavelets at scale $a = b = 0.2$.

Spherical wavelet transform

- Motion on the sphere (\equiv rotation)

$$[R(\rho)s](\omega) = s(\rho^{-1}\omega), \quad \rho \in \text{SO}(3)$$

- Wavelet basis on the sphere

$$\{\psi_{a,b,\rho} \equiv R(\rho)\mathcal{D}(a,b)\psi, \quad \rho \in \text{SO}(3), a, b \in \mathbb{R}_*^+\}$$

- Spherical wavelet transform

$$W_\psi(a, b, \rho) \equiv \int_{S^2} d\Omega(\omega) \psi_{a,b,\rho}^*(\omega) s(\omega)$$

- Fast algorithm (McEwen et al. 2005; Wandelt & Gorski 2001)

Spherical wavelet transform

- Motion on the sphere (\equiv rotation)

$$[R(\rho)s](\omega) = s(\rho^{-1}\omega), \quad \rho \in \text{SO}(3)$$

- Wavelet basis on the sphere

$$\{\psi_{a,b,\rho} \equiv R(\rho)\mathcal{D}(a,b)\psi, \quad \rho \in \text{SO}(3), \quad a, b \in \mathbb{R}_*^+\}$$

- Spherical wavelet transform

$$W_\psi(a, b, \rho) \equiv \int_{S^2} d\Omega(\omega) \psi_{a,b,\rho}^*(\omega) s(\omega)$$

- Fast algorithm (McEwen et al. 2005; Wandelt & Gorski 2001)

Spherical wavelet transform

- Motion on the sphere (\equiv rotation)

$$[R(\rho)s](\omega) = s(\rho^{-1}\omega), \quad \rho \in \text{SO}(3)$$

- Wavelet basis on the sphere

$$\{\psi_{\mathbf{a},\mathbf{b},\rho} \equiv R(\rho)\mathcal{D}(\mathbf{a},\mathbf{b})\psi, \quad \rho \in \text{SO}(3), \mathbf{a}, \mathbf{b} \in \mathbb{R}_*^+\}$$

- Spherical wavelet transform

$$W_\psi(\mathbf{a}, \mathbf{b}, \rho) \equiv \int_{S^2} d\Omega(\omega) \psi_{\mathbf{a},\mathbf{b},\rho}^*(\omega) s(\omega)$$

- Fast algorithm (McEwen et al. 2005; Wandelt & Gorski 2001)

Spherical wavelet transform

- Motion on the sphere (\equiv rotation)

$$[R(\rho)s](\omega) = s(\rho^{-1}\omega), \quad \rho \in \text{SO}(3)$$

- Wavelet basis on the sphere

$$\{\psi_{\mathbf{a},\mathbf{b},\rho} \equiv R(\rho)\mathcal{D}(\mathbf{a},\mathbf{b})\psi, \quad \rho \in \text{SO}(3), \mathbf{a}, \mathbf{b} \in \mathbb{R}_*^+\}$$

- Spherical wavelet transform

$$W_\psi(\mathbf{a}, \mathbf{b}, \rho) \equiv \int_{S^2} d\Omega(\omega) \psi_{\mathbf{a},\mathbf{b},\rho}^*(\omega) s(\omega)$$

- Fast algorithm (McEwen et al. 2005; Wandelt & Gorski 2001)

Outline

- 1 Integrated Sachs-Wolfe (ISW) effect
 - Physical origin
 - Detecting the effect
- 2 The continuous spherical wavelet transform (CSWT)
 - Dilations and mother wavelets on the sphere
 - Transform
- 3 Cross-correlation in wavelet space**
 - Wavelet covariance estimator**
 - Comparison of wavelets**
- 4 Analysis procedure
- 5 Results
 - Detections
 - Dark energy constraints
- 6 Summary

Wavelet covariance estimator

- Suitability of wavelets for detecting cross-correlations
- Wavelet covariance

$$\hat{X}_{\psi}^{\text{NT}}(a, b, \gamma) = \frac{1}{N_{\alpha\beta}} \sum_{\alpha, \beta} \nu_{\alpha\beta} W_{\psi}^{\text{N}}(a, b, \alpha, \beta, \gamma) W_{\psi}^{\text{T}}(a, b, \alpha, \beta, \gamma)$$

- Average over orientations

$$\hat{X}_{\psi}^{\text{NT}}(a, b) = \frac{1}{N_{\gamma}} \sum_{\gamma} \hat{X}_{\psi}^{\text{NT}}(a, b, \gamma)$$

- Theoretical wavelet covariance

$$X_{\psi}^{\text{NT}}(a, b, \gamma) = \sum_{\ell=0}^{\infty} p_{\ell}^2 b_{\ell}^{\text{N}} b_{\ell}^{\text{T}} C_{\ell}^{\text{NT}} \sum_{m=-\ell}^{\ell} |(\psi_{a,b})_{\ell m}|^2$$

Wavelet covariance estimator

- Suitability of wavelets for detecting cross-correlations
- Wavelet covariance

$$\hat{X}_{\psi}^{\text{NT}}(\mathbf{a}, \mathbf{b}, \gamma) = \frac{1}{N_{\alpha\beta}} \sum_{\alpha, \beta} \nu_{\alpha\beta} W_{\psi}^{\text{N}}(\mathbf{a}, \mathbf{b}, \alpha, \beta, \gamma) W_{\psi}^{\text{T}}(\mathbf{a}, \mathbf{b}, \alpha, \beta, \gamma)$$

- Average over orientations

$$\hat{X}_{\psi}^{\text{NT}}(\mathbf{a}, \mathbf{b}) = \frac{1}{N_{\gamma}} \sum_{\gamma} \hat{X}_{\psi}^{\text{NT}}(\mathbf{a}, \mathbf{b}, \gamma)$$

- Theoretical wavelet covariance

$$X_{\psi}^{\text{NT}}(\mathbf{a}, \mathbf{b}, \gamma) = \sum_{\ell=0}^{\infty} p_{\ell}^2 b_{\ell}^{\text{N}} b_{\ell}^{\text{T}} C_{\ell}^{\text{NT}} \sum_{m=-\ell}^{\ell} |(\psi_{\mathbf{a}, \mathbf{b}})_{\ell m}|^2$$

Wavelet covariance estimator

- Suitability of wavelets for detecting cross-correlations
- Wavelet covariance

$$\hat{X}_{\psi}^{\text{NT}}(\mathbf{a}, \mathbf{b}, \gamma) = \frac{1}{N_{\alpha\beta}} \sum_{\alpha, \beta} \nu_{\alpha\beta} W_{\psi}^{\text{N}}(\mathbf{a}, \mathbf{b}, \alpha, \beta, \gamma) W_{\psi}^{\text{T}}(\mathbf{a}, \mathbf{b}, \alpha, \beta, \gamma)$$

- Average over orientations

$$\hat{X}_{\psi}^{\text{NT}}(\mathbf{a}, \mathbf{b}) = \frac{1}{N_{\gamma}} \sum_{\gamma} \hat{X}_{\psi}^{\text{NT}}(\mathbf{a}, \mathbf{b}, \gamma)$$

- Theoretical wavelet covariance

$$X_{\psi}^{\text{NT}}(\mathbf{a}, \mathbf{b}, \gamma) = \sum_{\ell=0}^{\infty} p_{\ell}^2 b_{\ell}^{\text{N}} b_{\ell}^{\text{T}} C_{\ell}^{\text{NT}} \sum_{m=-\ell}^{\ell} |(\psi_{\mathbf{a}, \mathbf{b}})_{\ell m}|^2$$

Wavelet covariance estimator

- Suitability of wavelets for detecting cross-correlations
- Wavelet covariance

$$\hat{X}_{\psi}^{\text{NT}}(\mathbf{a}, \mathbf{b}, \gamma) = \frac{1}{N_{\alpha\beta}} \sum_{\alpha, \beta} \nu_{\alpha\beta} W_{\psi}^{\text{N}}(\mathbf{a}, \mathbf{b}, \alpha, \beta, \gamma) W_{\psi}^{\text{T}}(\mathbf{a}, \mathbf{b}, \alpha, \beta, \gamma)$$

- Average over orientations

$$\hat{X}_{\psi}^{\text{NT}}(\mathbf{a}, \mathbf{b}) = \frac{1}{N_{\gamma}} \sum_{\gamma} \hat{X}_{\psi}^{\text{NT}}(\mathbf{a}, \mathbf{b}, \gamma)$$

- Theoretical wavelet covariance

$$X_{\psi}^{\text{NT}}(\mathbf{a}, \mathbf{b}, \gamma) = \sum_{\ell=0}^{\infty} p_{\ell}^2 b_{\ell}^{\text{N}} b_{\ell}^{\text{T}} C_{\ell}^{\text{NT}} \sum_{m=-\ell}^{\ell} |(\psi_{\mathbf{a}, \mathbf{b}})_{\ell m}|^2$$

Comparison of wavelets

- Compare predicted signal-to-noise ratio

$$\text{SNR}_\psi(a, b) = \frac{\langle \hat{X}_\psi^{\text{NT}}(a, b) \rangle}{\Delta \hat{X}_\psi^{\text{NT}}(a, b)}$$

where

$$[\Delta \hat{X}_\psi^{\text{NT}}(a, b)]^2 = \sum_{\ell=0}^{\infty} \frac{1}{2\ell+1} \rho_\ell^4 (b_\ell^{\text{N}})^2 (b_\ell^{\text{T}})^2 \left(\sum_{m=-\ell}^{\ell} |(\psi_{a,b})_{\ell m}|^2 \right)^2 ((C_\ell^{\text{NT}})^2 + C_\ell^{\text{TT}} C_\ell^{\text{NN}})$$

- Similar technique used to compare real, harmonic and wavelet space techniques for detection of cross-correlations
→ wavelets optimal on certain scales (Vielva et al. 2005)

Comparison of wavelets

- Compare predicted signal-to-noise ratio

$$\text{SNR}_\psi(a, b) = \frac{\langle \hat{X}_\psi^{\text{NT}}(a, b) \rangle}{\Delta \hat{X}_\psi^{\text{NT}}(a, b)}$$

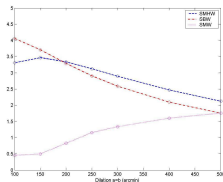
where

$$[\Delta \hat{X}_\psi^{\text{NT}}(a, b)]^2 = \sum_{\ell=0}^{\infty} \frac{1}{2\ell+1} \rho_\ell^4 (b_\ell^{\text{N}})^2 (b_\ell^{\text{T}})^2 \left(\sum_{m=-\ell}^{\ell} |(\psi_{a,b})_{\ell m}|^2 \right)^2 ((C_\ell^{\text{NT}})^2 + C_\ell^{\text{TT}} C_\ell^{\text{NN}})$$

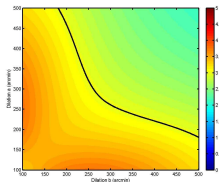
- Similar technique used to compare real, harmonic and wavelet space techniques for detection of cross-correlations
→ wavelets optimal on certain scales (Vielva et al. 2005)

Comparison of wavelets

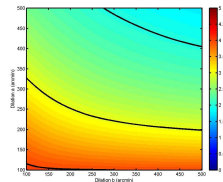
SNR plots



(a) All wavelets



(b) SMHW



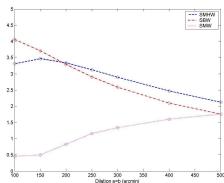
(c) SBW

Figure: Expected SNR of the wavelet covariance estimator of CMB and radio source maps

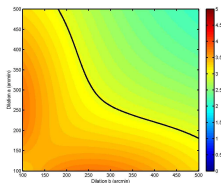
- Don't consider SMW further
(actually considered; as expected not effective)

Comparison of wavelets

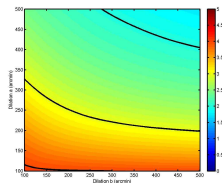
SNR plots



(a) All wavelets



(b) SMHW



(c) SBW

Figure: Expected SNR of the wavelet covariance estimator of CMB and radio source maps

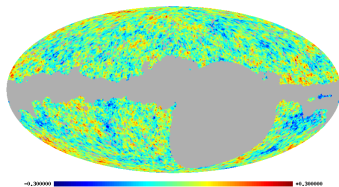
- Don't consider SMW further
(actually considered; as expected not effective)

Outline

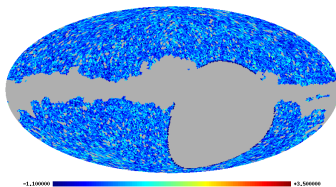
- 1 Integrated Sachs-Wolfe (ISW) effect
 - Physical origin
 - Detecting the effect
- 2 The continuous spherical wavelet transform (CSWT)
 - Dilations and mother wavelets on the sphere
 - Transform
- 3 Cross-correlation in wavelet space
 - Wavelet covariance estimator
 - Comparison of wavelets
- 4 **Analysis procedure**
- 5 Results
 - Detections
 - Dark energy constraints
- 6 Summary

Analysis procedure

- Data



WMAP

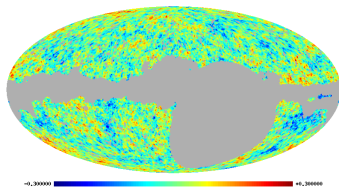


NVSS

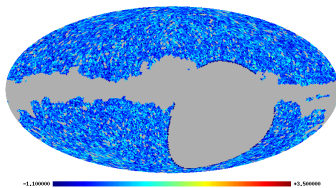
- Analysis (scales; masks)
- Simulations
- Constraints on dark energy parameters

Analysis procedure

- Data



WMAP

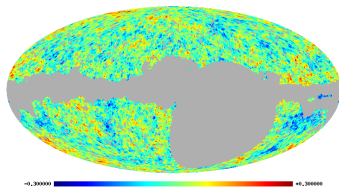


NVSS

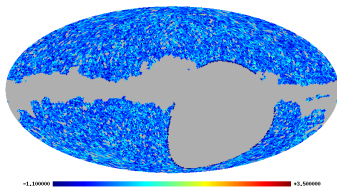
- Analysis (scales; masks)
- Simulations
- Constraints on dark energy parameters

Analysis procedure

- Data



WMAP

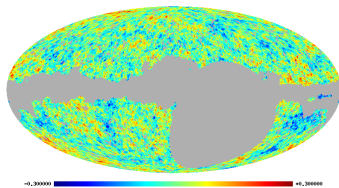


NVSS

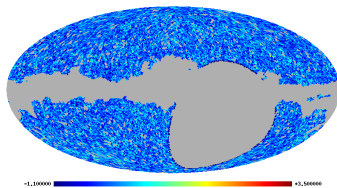
- Analysis (scales; masks)
- Simulations
- Constraints on dark energy parameters

Analysis procedure

- Data



WMAP



NVSS

- Analysis (scales; masks)
- Simulations
- Constraints on dark energy parameters

Outline

- 1 Integrated Sachs-Wolfe (ISW) effect
 - Physical origin
 - Detecting the effect
- 2 The continuous spherical wavelet transform (CSWT)
 - Dilations and mother wavelets on the sphere
 - Transform
- 3 Cross-correlation in wavelet space
 - Wavelet covariance estimator
 - Comparison of wavelets
- 4 Analysis procedure
- 5 Results**
 - Detections
 - Dark energy constraints
- 6 Summary

Scales and detections

- Scales

Scale	1	2	3	4	5	6	7
Dilation a	100'	150'	200'	250'	300'	400'	500'
Size on sky 1	282'	424'	565'	706'	847'	1130'	1410'
Size on sky 2	31.4'	47.1'	62.8'	78.5'	94.2'	126'	157'

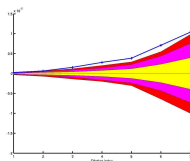
- Wavelet covariance plots

Scales and detections

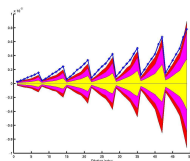
- Scales

Scale	1	2	3	4	5	6	7
Dilation a	100'	150'	200'	250'	300'	400'	500'
Size on sky 1	282'	424'	565'	706'	847'	1130'	1410'
Size on sky 2	31.4'	47.1'	62.8'	78.5'	94.2'	126'	157'

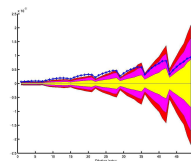
- Wavelet covariance plots



SMHW



SMHW



SBW

Significance of detections

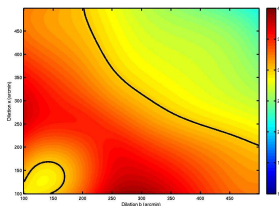
- Most significant detections
 - Wavelet covariance statistics appear Gaussian
 - N_σ direct indication of significance of detections
 - symmetric SMHW: 3.6σ ; elliptical SMHW: 3.9σ ; SBW: 3.9σ
- N_σ plots (2 and 3σ contours)

Significance of detections

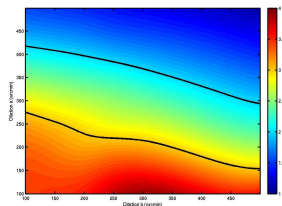
- Most significant detections
 - Wavelet covariance statistics appear Gaussian
 - N_σ direct indication of significance of detections
 - symmetric SMHW: 3.6σ ; elliptical SMHW: 3.9σ ; SBW: 3.9σ
- N_σ plots (2 and 3σ contours)

Significance of detections

- Most significant detections
 - Wavelet covariance statistics appear Gaussian
 - N_σ direct indication of significance of detections
 - symmetric SMHW: 3.6σ ; elliptical SMHW: 3.9σ ; SBW: 3.9σ
- N_σ plots (2 and 3σ contours)



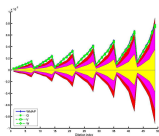
SMHW



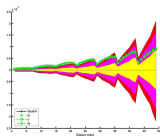
SBW

Systematics and foregrounds

- Systematics: individual WMAP receiver maps
→ systematics not likely source of detection
- Foregrounds: foreground dominated difference maps
→ foregrounds not likely source of detection



SMHW



SBW

Individual receiver maps

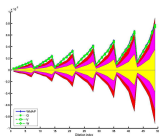
SMHW

SBW

Difference maps

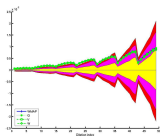
Systematics and foregrounds

- Systematics: individual WMAP receiver maps
→ systematics not likely source of detection
- Foregrounds: foreground dominated difference maps
→ foregrounds not likely source of detection

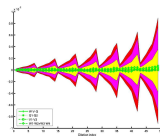


SMHW

Individual receiver maps

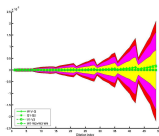


SBW



SMHW

Difference maps



SBW

Localised regions

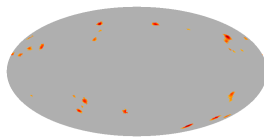
Detection

- Wavelets inherently provide spatial localisation (in addition to scale localisation)
- Threshold wavelet coefficient product maps to localise most likely sources

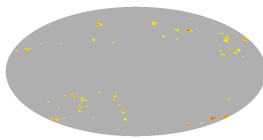
Localised regions

Detection

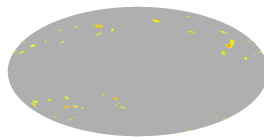
- Wavelets inherently provide spatial localisation (in addition to scale localisation)
- Threshold wavelet coefficient product maps to localise most likely sources



Symmetric SMHW



Elliptical SMHW

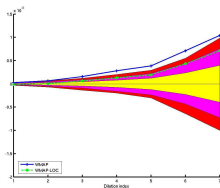


SBW

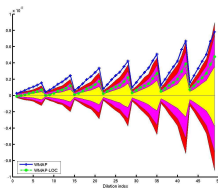
Localised regions

Removal

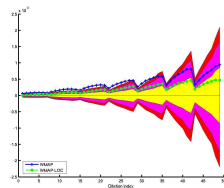
- Remove localised regions → ISW detection remains
(Agrees with findings of Boughn and Crittenden 2004)



Symmetric SMHW



Elliptical SMHW



SBW

Dark energy constraints

- Compute theoretical wavelet covariance for range of models (w, Ω_Λ)
(assume concordance model for other parameters; bias $b = 1.6$)
- Compare theoretical predictions with observations

$$\chi^2(w, \Omega_\Lambda) = \Delta^T C^{-1} \Delta$$

where

$$\Delta = [\hat{X}_\psi^{\text{NT}}(a, b, \gamma) - X_\psi^{\text{NT}}(a, b, \gamma | w, \Omega_\Lambda)]$$

- Compute likelihood

$$\mathcal{L}(w, \Omega_\Lambda) \propto \exp[-\chi^2(w, \Omega_\Lambda)/2]$$

Dark energy constraints

- Compute theoretical wavelet covariance for range of models (w, Ω_Λ)
(assume concordance model for other parameters; bias $b = 1.6$)
- Compare theoretical predictions with observations

$$\chi^2(w, \Omega_\Lambda) = \Delta^T \mathbf{C}^{-1} \Delta$$

where

$$\Delta = [\hat{X}_\psi^{\text{NT}}(a, b, \gamma) - X_\psi^{\text{NT}}(a, b, \gamma | w, \Omega_\Lambda)]$$

- Compute likelihood

$$\mathcal{L}(w, \Omega_\Lambda) \propto \exp[-\chi^2(w, \Omega_\Lambda)/2]$$

Dark energy constraints

- Compute theoretical wavelet covariance for range of models (w, Ω_Λ)
(assume concordance model for other parameters; bias $b = 1.6$)
- Compare theoretical predictions with observations

$$\chi^2(w, \Omega_\Lambda) = \Delta^T C^{-1} \Delta$$

where

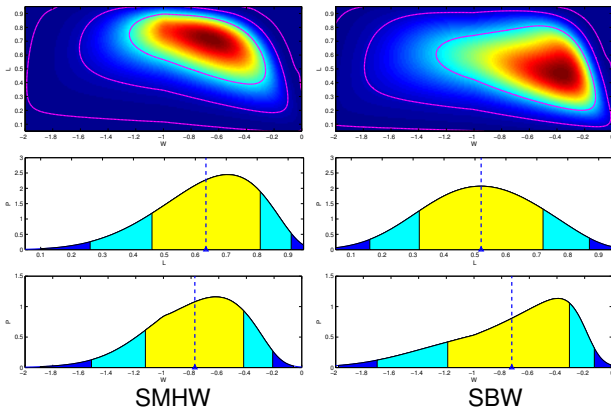
$$\Delta = [\hat{X}_\psi^{\text{NT}}(a, b, \gamma) - X_\psi^{\text{NT}}(a, b, \gamma | w, \Omega_\Lambda)]$$

- Compute likelihood

$$\mathcal{L}(w, \Omega_\Lambda) \propto \exp[-\chi^2(w, \Omega_\Lambda)/2]$$

Dark energy constraints

Likelihood surfaces (preliminary)



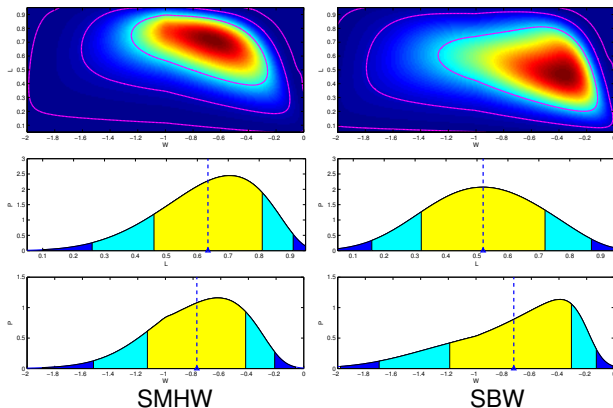
- Parameter estimates from mean of marginalised distributions

- $\Omega_\Lambda = 0.63^{+0.18}_{-0.17}$, $w = -0.77^{+0.35}_{-0.36}$ using SMHW

- $\Omega_\Lambda = 0.52^{+0.20}_{-0.20}$, $w = -0.73^{+0.42}_{-0.46}$ using SBW

Dark energy constraints

Likelihood surfaces (preliminary)

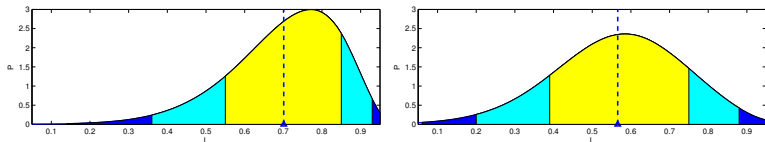


- Parameter estimates from mean of marginalised distributions

- $\Omega_\Lambda = 0.63^{+0.18}_{-0.17}$, $w = -0.77^{+0.35}_{-0.36}$ using SMHW
- $\Omega_\Lambda = 0.52^{+0.20}_{-0.20}$, $w = -0.73^{+0.42}_{-0.46}$ using SBW

Dark energy constraints

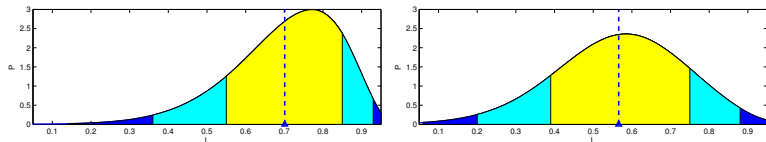
Parameter estimates (preliminary)



- Also considered case $w = -1$
 - $\Omega_\Lambda = 0.70^{+0.15}_{-0.15}$ using SMHW
 - $\Omega_\Lambda = 0.57^{+0.18}_{-0.18}$ using SBW
- Reject $\Omega_\Lambda = 0$ at $> 99\%$ significance
 - $\Omega_\Lambda > 0.1$ at 99.9% using SMHW
 - $\Omega_\Lambda > 0.1$ at 99.7% using SBW

Dark energy constraints

Parameter estimates (preliminary)



- Also considered case $w = -1$
 - $\Omega_\Lambda = 0.70^{+0.15}_{-0.15}$ using SMHW
 - $\Omega_\Lambda = 0.57^{+0.18}_{-0.18}$ using SBW
- Reject $\Omega_\Lambda = 0$ at $> 99\%$ significance
 - $\Omega_\Lambda > 0.1$ at 99.9% using SMHW
 - $\Omega_\Lambda > 0.1$ at 99.7% using SBW

Outline

- 1 Integrated Sachs-Wolfe (ISW) effect
 - Physical origin
 - Detecting the effect
- 2 The continuous spherical wavelet transform (CSWT)
 - Dilations and mother wavelets on the sphere
 - Transform
- 3 Cross-correlation in wavelet space
 - Wavelet covariance estimator
 - Comparison of wavelets
- 4 Analysis procedure
- 5 Results
 - Detections
 - Dark energy constraints
- 6 Summary

Summary

- Using spherical wavelets to detect ISW effect
- Detection of ISW effect made at almost 4σ
- Independent evidence of dark energy
- Constrain dark energy

Summary

- Using spherical wavelets to detect ISW effect
- Detection of ISW effect made at almost 4σ
- Independent evidence of dark energy
- Constrain dark energy

Summary

- Using spherical wavelets to detect ISW effect
- Detection of ISW effect made at almost 4σ
- Independent evidence of dark energy
- Constrain dark energy